Low-Temperature Synthesis of $Mg_xCo_{1-x}Co_2O_4$ Spinel Catalysts for N_2O Decomposition

U. Chellam, Z. P. Xu, and H. C. Zeng*

Department of Chemical and Environmental Engineering, Faculty of Engineering National University of Singapore, 10 Kent Ridge Crescent, Singapore 119260

Received June 4, 1999. Revised Manuscript Received December 16, 1999

Low-temperature synthesis of spinels $Mg_xCo_{1-x}Co_2O_4$ ($x = 0.0-0.9$) has been investigated with two important synthetic parameters and XRD/FTIR/DSC/BET/ICP/CHN methods. It is found that with an increase in hydrothermal treatment temperature, precursor compounds change from the hydrotalcite-like to brucite-like and then to cubic spinel phase when the initial metal concentration ratio $[Mg^{2+}]:[Co^{2+}] \geq 1$, while from the turbostratic to hydrotalcite-like and then to cubic spinel phase when the $[Mg^{2+}]:[Co^{2+}] < 1$. The $Mg_xCo_{1-x}Co_2O_4$ ($x \leq {}^1/_3$) spinels were formed at temperatures as low as 50−100 °C. In the postsynthesis thermal treatment, various thermal events have been observed, and in all cases the spinel phase can be prepared at temperatures below 300 °C. On the basis of FTIR results, a topotactic mechanism for the formation of the spinel phase has been confirmed. Specific surface area as high as 210 m^2/g has been attained in 400 °C calcined $Mg_xCo_{1-x}Co_2O_4$ with $x = 0.9$. Causes for the formation of the spinel phase at low temperatures have been addressed. Excellent catalytic activity for N_2O decomposition (30.6−38.9 mmol $(N_2O)/g{\cdot}h$ at GHSV = 21200 h^{-1} and 380−400 °C; N_2O = 10 mol % balanced with He) has been observed and discussed for these Mg−Co spinels.

Introduction

In recent years, oxide spinels of 3d transition metals have been the subject of increasing fundamental and applied research because of their special electric, magnetic, and catalytic properties.[1−9] It is known that the synthetic process of spinel precursor compounds, which determines final oxide structure, texture, and chemical composition, plays a crucial role in ultimate performance of these spinels.[5,9]

Spinel oxides belong to a class of complex oxides with the chemical formulas of AB_2O_4 in which A ions are generally divalent cations occupying tetrahedral sites and B ions are trivalent cations in octahedral sites. The cobalt oxide spinel Co_3O_4, for example, is one receiving considerable interest.[10−15] The Co_3O_4 consists of two distinct types of cobalt ions, Co^{2+} ($3d^7$) in the tetrahedral sites and Co^{3+} ($3d^6$) in the octahedral sites, with a Co^{2+}:Co^{3+} ratio of 1:2.[10] For the electronic configurations, the former (Co^{2+}) is an $(e_g)^4(t_{2g})^3$ system in a tetrahedral field with $S = {}^3/_2$ and the latter (Co^{3+}) has a $(t_{2g})^6$ structure and is diamagnetic ($S = 0$). It should be mentioned that in the normal spinel structure, the divalent Co^{2+} is connected only to four nearest neighboring oxygen anions. In fact, the divalent Co^{2+} can be further coordinated to the oxygen anions up to a maximum of six, as in the CoO phase where the Co^{2+} ions occupy octahedral sites formed by six oxygen anions (rock salt structure) and the $3d^7$ electrons are located as $(t_{2g})^5(e_g)^2$ configurations and with spin $S = {}^3/_2$. Accordingly, the chemical reactivity of a Co^{2+} in a tetrahedral site and octahedral site should be different because of differences in their respective geometrical and electronic configurations.

The A component of the spinel oxide Co_3O_4 (or $CoCo_2O_4$) is often substituted partially with other divalent 3d transition metals such as Cr, Mn, Ni, Cu, and Zn, and/or earth alkali metals such as Mg to create special chemicophysical properties for a specific application.[1−9] With regard to their applications in catalysis, for example, it has been known that the catalytic activity of these spinels depends essentially on two factors: the degree of A substitution and the degree of inversion of the spinel. These two material parameters in turn depend heavily on the synthetic approach and postsynthesis treatment of the precursor compounds.[2,5,9]

* Corresponding author. Telephone: +65 874 2896. Telefax: +65 779 1936. E-mail: chezhc@nus.edu.sg.

(1) Petrov, K.; Will, G. *J. Mater. Sci. Lett.* **1987**, *6*, 1153.
(2) Petrov, K.; Markov, L.; Rachev, P. *React. Solids* **1987**, *3*, 67.
(3) Zotov, N.; Petrov, K.; Dimitrova-Pankova, M. *J. Phys. Chem. Solids* **1990**, *51*, 1199.
(4) Markov, L.; Petrov, K.; Lyubchova, A. *Solid State Ionics* **1990**, *39*, 187.
(5) Markov, L.; Lyubchova, A. *J. Mater. Sci. Lett.* **1991**, *10*, 512.
(6) Rojas, R. M.; Vila, E.; Garcia-Martinez, O.; Martin de Vidales, J. L. *J. Mater. Chem.* **1994**, *4*, 1635.
(7) Martin de Vidales, J. L.; Vila, E.; Rojas, R. M.; Garcia-Martinez, O. *Chem. Mater.* **1995**, *7*, 1716.
(8) Rios, E.; Poillerat, G.; Koenig, J. F.; Gautier, J. L.; Chartier, P. *Thin Solid Films* **1995**, *264*, 18.
(9) Qian, M.; Zeng, H. C. *J. Mater. Chem.* **1997**, *7*, 493.
(10) Kim, K. S. *Phys. Rev. B* **1975**, *11*, 2178.
(11) Chuang, T. J.; Brundle, C. R.; Rice, D. W. *Surf. Sci.* **1976**, *59*, 413.
(12) Mitton, D. B.; Walton, J.; Thompson, G. E. *Surf. Interface Anal.* **1993**, *20*, 36.
(13) McIntyre, N. S.; Johnston, D. D.; Coatsworth, L. L.; Davidson, R. D. *Surf. Interface Anal.* **1990**, *15*, 265.
(14) Oku, M.; Sato, Y. *Appl. Surf. Sci.* **1992**, *55*, 37.
(15) Xu, Z. P.; Zeng, H. C. *J. Mater. Chem.* **1998**, *8*, 2499.

10.1021/cm990355l CCC: $19.00
Published on Web 02/22/2000

Table 1. Preparation Conditions and Spinel Formulas

sample	$[Mg^{2+}]:[Co^{2+}]^a$	T,[b] °C	final pH[c]	$Mg_xCo_{1-x}Co_2O_4$[d]	γ[e]
A25	2:1	25	8.5	$Mg_{0.81}Co_{0.19}Co_2O_4$	0.54
A50	2:1	50	7.0	$Mg_{0.83}Co_{0.17}Co_2O_4$	0.55
A75	2:1	75	6.5	$Mg_{0.91}Co_{0.09}Co_2O_4$	0.61
A100	2:1	100	6.5	$Mg_{0.33}Co_{0.67}Co_2O_4$	0.22
B25	1:1	25	8.0	$Mg_{0.34}Co_{0.66}Co_2O_4$	0.23
B50	1:1	50	7.0	$Mg_{0.48}Co_{0.52}Co_2O_4$	0.32
B75	1:1	75	6.5	$Mg_{0.69}Co_{0.28}Co_2O_4$	0.46
B100	1:1	100	6.5	$CoCo_2O_4(Co_3O_4)$	
C25	1:2	25	8.0	$Mg_{0.14}Co_{0.86}Co_2O_4$	0.09
C50	1:2	50	7.0	$Mg_{0.23}Co_{0.77}Co_2O_4$	0.15
C75	1:2	75	6.5	$Mg_{0.35}Co_{0.65}Co_2O_4$	0.23
C100	1:2	100	6.5	$CoCo_2O_4$ (Co_3O_4)	

[a] $[Mg^{2+}]:[Co^{2+}]$ is mole ratio of Mg^{2+} to Co^{2+} in the initial mixed metal solutions. [b] Temperature used during the hydrothermal aging of hydroxides. [c] pH value of mother liquid after hydrothermal aging at respective temperature for 24 h. [d] Spinel formula for the as prepared samples after calcination at 400°C for 2 h, based on the elemental analysis data in Table 2. [e] γ is the theoretical degree of inversion (see text) in the cationic distribution formula $(Mg_{x-\gamma}{}^{2+}Co_{1-x}{}^{2+}Co_\gamma{}^{3+})^{Td}[Mg_\gamma{}^{2+}Co_{2-\gamma}{}^{3+}]^{Oh}O_4$, noting that the x values are indicated in d).

In this paper, we will use a new hydrothermal approach to synthesize $Mg_xCo_{1-x}Co_2O_4$ spinels under oxygen atmosphere (1 atm) for N_2O decomposition. Present findings indicate that both the degree of A substitution and the degree of inversion can be adjusted by selecting initial metal concentration ratio of $[Mg^{2+}]/[Co^{2+}]$ and hydrothermal treatment temperature.

Experimental Section

Materials Preparation. Magnesium−cobalt hydroxides were prepared using a coprecipitation method. Briefly, 60.0 mL of 1.0 M mixed-metal nitrate aqueous solution of Mg^{2+} and Co^{2+} ($Mg(NO_3)_2{\cdot}6H_2O$, > 99.0%, Merck; $Co(NO_3)_2{\cdot}6H_2O$, > 99.0%, Fluka) with various metal mole ratios was added into 300.0 mL of 0.5 M ammoniacal solution (pH = 10.5) in a three-necked round-bottom flask within 1 min. The addition and precipitation were carried out under magnetic stirring and ambient control with purified oxygen gas (Soxal, O_2 > 99.8%) bubbling through the solution at a rate of 25 mL/min at room temperature (25 °C). The resulting precipitate was hydrothermally treated (i.e., aged) at a selected temperature (25−100 °C) while stirring under the O_2 at normal atmospheric pressure. A reflux unit was mounted on the top of the flask to prevent water and ammonia from escaping. After the hydrothermal treatment, the aged precipitate was filtered and washed thoroughly with deionized water, followed by drying at room temperature overnight in a vacuum. Final pH values of the filtrate were in the range of 8.5−6.5 depending on the starting metal composition and the selected temperature. Table 1 reports synthetic conditions and nomenclature for each precipitate sample.

Materials Characterization. Crystallographic information on the samples was established by powder X-ray diffraction (XRD) methods. Diffraction patterns of intensity versus two-theta (2θ) were recorded with a Shimadzu XRD-6000 X-ray diffractometer with Cu Kα radiation (λ = 1.5418 Å) from 8° to 40° at a scanning speed of 3°/min. Chemical bonding information on metal−oxygen, hydroxyl, and intercalated functional groups (such as nitrate anions) were investigated with Fourier transform infrared spectroscopy (FTIR, Shimadzu FTIR-8101) using the potassium bromide (KBr) pellet technique. High-purity KBr powder had been carefully dried before use to eliminate possible interference of retained water or hydroxyl groups to the samples. Each FTIR spectrum was collected after 100 scans with a resolution of 2.0 cm^{-1}.

The elemental analysis for metal species, Mg and Co, was done using inductively coupled plasma emission spectroscopy (Perkin-Elmer ICP OPTIMA-300). Contents of nonmetal elements such as nitrogen and carbon were measured using a CHN analyzer (Perkin-Elmer CHN EA-2400).

The thermal behavior of the Mg−Co hydroxides was investigated by differential scanning calorimetry and thermogravimetric analysis (Netzch DSC-200 and Shimadzu TGA-50). The samples were heated from 30 to 450 °C at a scanning rate of 10 °C/min under nitrogen atmosphere with a flow rate of 15 mL/min. The as-prepared precipitates were also heat-treated at 100, 200, 300, and 400 °C respectively for 2 h with static laboratory air in an electric furnace (Carbolite). Specific surface areas of the 400 °C calcined samples were determined by multipoint BET method in a Nova-1000 Instrument. Prior to N_2 adsorption−desorption measurement, each sample was degassed with N_2 purge at 350 °C for 3 h.

In catalytic activity tests, the as-prepared samples were air-calcined at 400 °C for 2 h, which were then vacuum-pressed into pellets under an external pressure of 8 tons/cm^2. The pellets were divided and screened into 44−60 mesh catalysts. About 155 mg of catalyst was used in a tubular quartz rector (inner diameter = 0.420−0.458 cm, catalyst volume V = 0.083−0.096 mL) in each run. The catalysts were activated at 350 °C overnight in a N_2O stream (10 mol %, balanced with He) with a flow rate of 35 mL/min. In a typical experiment, N_2O gas (10 mol %, balanced with He) was fed at a rate of 35 mL/min (F) through the catalyst bed at 1 atm. The GHSV was in the range of 21600−25200 h^{-1}. The outlet gases, cooled in a coil, were analyzed by gas chromatography (GC) on a Perkin-Elmer AutoSystem-XL (TCD detector) using a 4-foot Porapak Q (80/100 mesh). The catalytic activity for N_2O decomposition was evaluated in terms of conversion percentage

$$X = (P_{i,N_2O}-P_{f,N_2O})/(P_{i,N_2O}+0.5P_{i,N_2O}P_{f,N_2O})$$

where P_{i,N_2O} and P_{f,N_2O} are inlet and outlet partial pressures of nitrous oxide.[16]

Results and Discussion

Structural Phases of Precursors upon Reaction Conditions. Two major experimental variables considered in this work (Table 1) are (i) cation ratios of Mg^{2+} to Co^{2+} in starting metal solution and (ii) hydrothermal treatment temperature. Figure 1 shows the XRD patterns of the as-prepared samples under the conditions detailed in Table 1. As can be seen, the 25 °C prepared precipitates change from a hydrotalcite-like phase[17−19] (A25 and B25) to a turbostratic phase (C25) due to the difference in cation ratio.[20]

It should be mentioned that for a series of samples, within which the only preparative variable is temperature for hydrothermal aging, the starting precipitates should be the same since all the coprecipitation experiments were conducted at 25 °C. The hydrothermal treatment indeed creates great difference in final structures of the samples. As shown in Figure 1a, the 25 °C and 50 °C prepared samples of A series are in the HTlc phase and some of which is converted to brucite-like phase of hydroxides at 75 °C (A75).[21−23] With a higher

(16) Li, K.; Wang, X. F.; Zeng, H. C. *Chem. Eng. Res. Des. Part A: Trans. 1. Chem. E.* **1997**, *75*, 807.
(17) Cavani, F.; Trifiro, F.; Vaccari, A. *Catal. Today* **1991**, *11*, 173.
(18) Reichle, W. T. *Solid State Ionics* **1986**, *22*, 135.
(19) Labajos, F. M.; Rives, V. *Inorg. Chem.* **1996**, *35*, 5313.
(20) Tekaia Ehlsissen, K.; Delahaya-Vidal, A.; Genin, P.; Figlarz, M.; Willmann, P. *J. Mater. Chem.* **1993**, *3*, 883.
(21) Faure, C.; Delmas, C.; Fousassier, M. *J. Power Sources* **1991**, *35*, 279.
(22) Kamath, P. V.; Therese, G. H. A. *J. Solid State Chem.* **1997**, *128*, 38.
(23) Zeng, H. C.; Qian, M.; Xu, Z. P. *Chem. Mater.* **1998**, *10*, 2277.

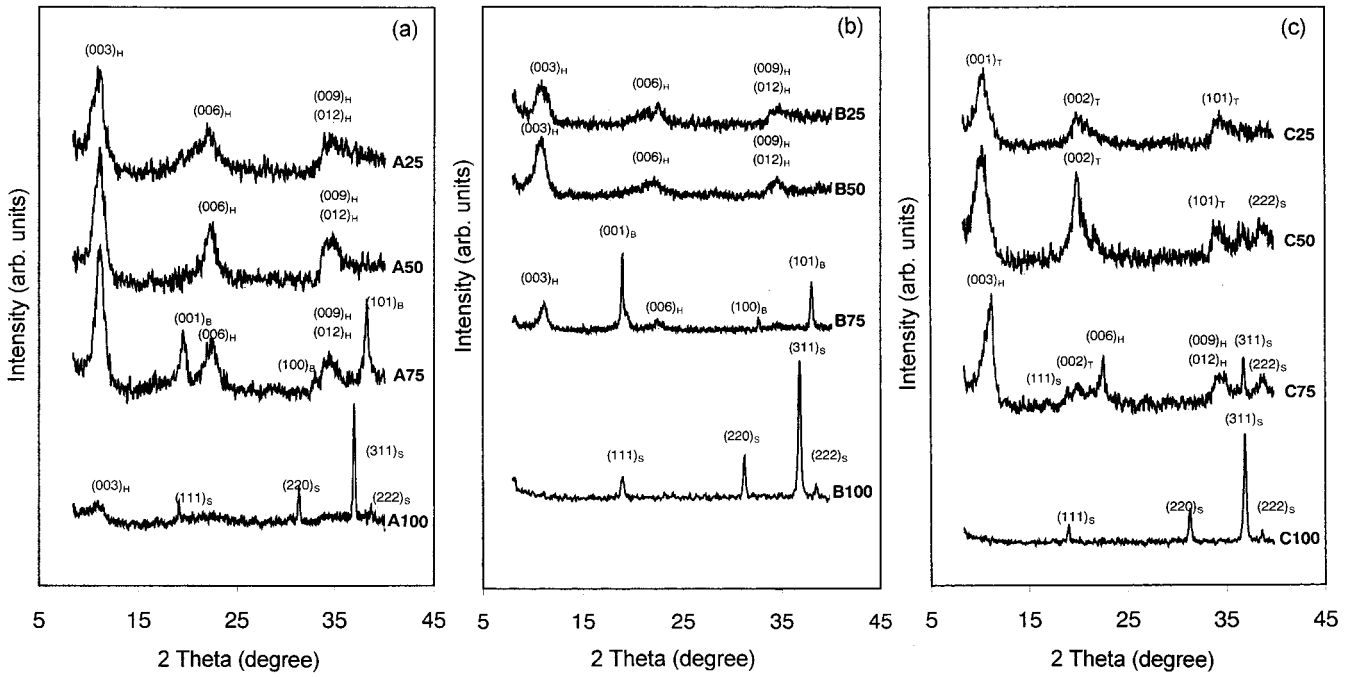

Figure 1. XRD patterns for the as-prepared precursor samples: (a) A series, (b) B series, and (c) C series. Subscript H stands for hydrotalcite-like phase; B, for brucite-like phase; S, for spinel phase; and T, for turbostratic phase.

Table 2. Elemental Analysis results from CHN and ICP Measurements

sample	CO_3^{2-} [a] (wt %)	NO_3^- [a] (wt %)	[b] NO_3^-/CO_3^{2-}	Mg[a] (wt %)	Co[a] (wt %)	Co/Mg[b]
A25	2.0	13.6	6.6	5.38	35.29	2.7
A50	2.0	15.5	7.5	6.38	40.62	2.6
A75	1.7	12.5	7.3	7.29	40.55	2.3
A100	0.9	10.0	10.7	2.04	40.07	8.1
B25	3.1	14.0	4.4	2.33	43.90	7.8
B50	1.9	15.4	7.8	2.97	37.68	5.2
B75	1.4	8.0	5.5	5.18	41.74	3.3
B100	0.4	0.0	0.0	0.0	62.26	∞
C25	2.2	14.2	6.2	0.89	44.27	20.5
C50	1.1	15.3	14.1	1.56	44.79	11.8
C75	1.6	14.0	8.7	2.41	44.39	7.6
C100	0.6	0.9	1.6	0.0	73.02	∞

[a] Weight % (wt %) is with respect to the sample weight on wet basis. [b] NO_3^-/CO_3^{2-} and Co/Mg are mole ratios in the as-prepared samples.

temperature at 100 °C, the resultant product is mainly in cubic spinel phase,[2,5−7] although the HTlc phase is still detectable. For the sample series B (Figure 1b), whose $[Mg^{2+}]$:$[Co^{2+}]$ ratio is reduced, the brucite-like phase in the 75 °C prepared sample is more pronounced, in addition to the presence of HTlc phase. When an aging temperature of 100 °C is applied, the product is in spinel phase (hydrous, Table 2, Co wt % = 62.26%).[15] When the $[Mg^{2+}]$:$[Co^{2+}]$ ratio is further reduced (the sample series C, Figure 1c), the spinel phase can be detected at an aging temperature as low as 50 °C (C50). Unlike the previous two series, the brucite-like phase is not observed. Single-phase spinel can be obtained at 100 °C in the C series (C100), noting that the Co wt % in Table 2 matches perfectly with the theoretical value of Co_3O_4.[15]

Elemental analysis reported in Table 2 on the above precipitate samples are in good agreement with the above XRD analysis. For the samples having a HTlc or turbostratic phase, the total content of NO_3^- and CO_3^{2-} is high due to the intercalation of anionic species in the inter-brucite-like layer spacing, while for the single phase spinel sample, such as B100 and C100, the anion content is virtually negligible. Within each series, the Co/Mg mole ratio in the precursor samples is constantly decreased before the hydrothermal treatment at 100 °C. Interestingly, the Mg content is substantially reduced in the 100 °C prepared samples. In particular, the Co/Mg ratio climbs suddenly to 8.1 in the sample A100 while the Mg content is undetected in the samples B100 and C100. In fact, both B100 and C100 are single-phase oxide spinel Co_3O_4.[15] It is believed that the original Mg cations are leached out of the precipitates when the mixed Mg−Co-hydroxides are hydrothermally decomposed at this temperature. Under current experimental conditions, it is recognized that the temperature for obtaining hydrothermally prepared $Mg_xCo_{1-x}Co_2O_4$ spinels is closely related to the Mg content in precipitates. If $x \leq 1/3$ (Table 1, or Table 2, Co/Mg ≥ 8), the $Mg_xCo_{1-x}Co_2O_4$ spinels can be obtained in the temperature range of 50−100 °C, as have been illustrated in the cases of C50, C75, and A100.

From the sample A25 to A100, FTIR spectra of Figure 2 change substantially noting that all samples contain the HTlc phase. The presence of interlayer NO_3^- is indicated in the sharp absorption peak at 1388 cm^{-1} (ν_3 mode), and the presence of CO_3^- anion can be observed in a small shoulder at ∼1356 cm^{-1}.[24,25] It is found that the ν_3 mode of nitrate ion departs from that at 1340−1380 cm^{-1} for an unperturbed NO_3^-.[25] In connection with this, ν_2 vibrational mode of the anion is also observable at 833 cm^{-1}.[25,26] In view of simultaneous observation of ν_2 and ν_3 modes of D_{3h} symmetry, it can be concluded that the anions have a planar configuration, although they have been slightly perturbed by their

(24) Chisem, I. C.; Jones, W. *J. Mater. Chem.* **1994**, *4*, 1737.
(25) Kruissink, E.; van Reijen, L. L.; Ross, J. R. H. *J. Chem. Soc., Faraday Trans. 1* **1981**, *77*, 649.
(26) Fernandez, J. M.; Barriga, C.; Ulibarri, M. A.; Labajos, F. M.; Rives, V. *J. Mater. Chem.* **1994**, *4*, 1117.

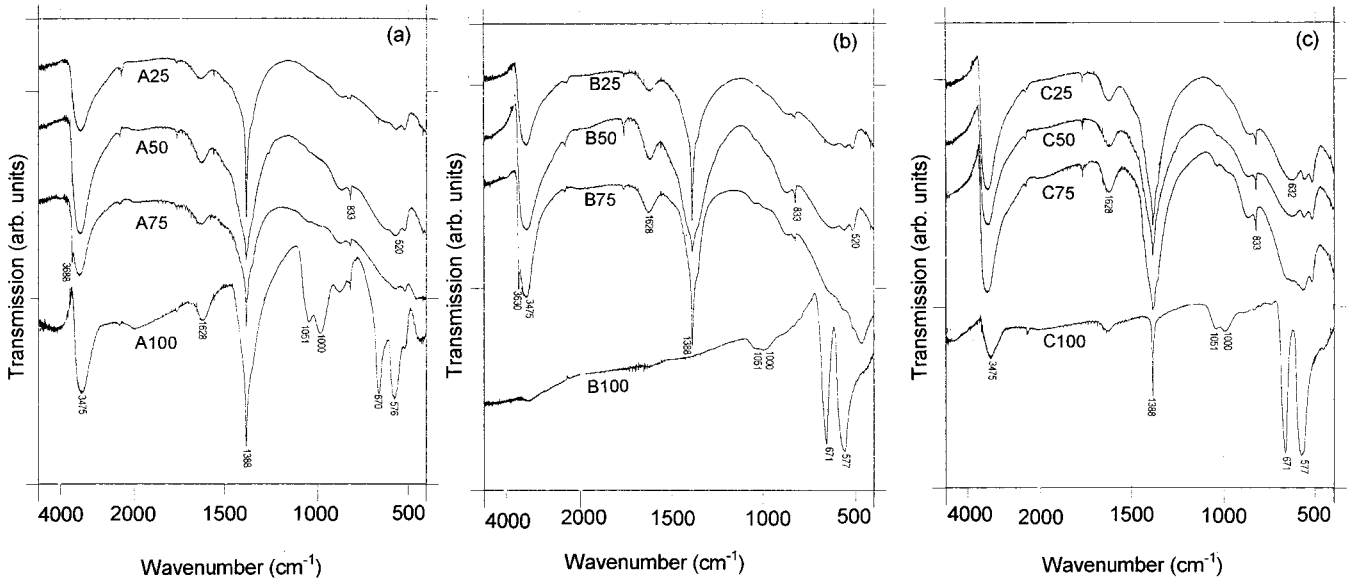

Figure 2. FTIR spectra for the as prepared precursor samples: (a) A series, (b) B series, and (c) C series.

adjacent chemical entities. The absorption peaks at 500−550 cm^{-1} can be attributed to metal−oxygen bond vibrations in the mixed-metal hydroxides.[27,28] In agreement with the HTlc structure, a broad peak arising from O−H vibrations of intercalated water and hydroxyl groups of HTlc phase is located at ∼3475 cm^{-1} in all spectra of this series. It is noted that this peak is blue-shifted from the earlier reported ones (3449−3455 cm^{-1}),[23] indicating an increase of basicity for the O−H group. The bending mode of water molecule δ_{H-O-H} can be observed at 1628 cm^{-1}. For the sample A75, a high wavenumber O−H peak at 3688 cm^{-1} is also observed, due to the presence of brucite-like phase in the sample (Figure 1).[28−30] In the 100 °C prepared sample A100, characteristic spinel IR absorption peaks are observed at 670 and 576 cm^{-1} respectively.[9,15,31] It is recognized that a conversion of HTlc to spinel phase takes place at 100 °C since the HTlc phase diffraction peaks are becoming weaker while the intensity of spinel phase diffraction peaks is increased sharply (Figure 1). This process is also reflected in FTIR spectrum of A100 (Figure 2a). While converted into the spinel phase, the anions (NO_3^- and CO_3^{2-}) in the HTlc phase are distorted and lowered their symmetry from D_{3h} to C_{2v}, resulting in the observable IR vibrational absorption mode (ν_2 mode in C_{2v} symmetry) of the anions at 1051−1000 cm^{-1}.[20,24−26]

In IR spectra for the sample series B, high wavenumber O−H peak at 3630 cm^{-1} can be observed in the brucite-like-phase-containing sample B75, whose preparation temperature is identical to that of A75. However, the IR spectrum of sample B100 is totally different from the rest. For example, the D_{3h}-related vibrations (1388 and 833 cm^{-1}) disappear, leaving only a small lump at 1051−1000 cm^{-1} (ν_2 mode, C_{2v}).[20,24−26] This is in good agreement with the XRD observation that there is no HTlc phase in B100 and the sample has been converted into spinel phase at 100 °C. As for the series C, the respective IR assignments can be done on the basis of the above analysis. Similar to the XRD results, the IR characteristic vibrations for spinel phase can be detected as early as in the C75, noting that the two absorption peaks are fully developed in C100.[9,15,31]

Formation of $Mg_xCo_{1-x}Co_2O_4$ Spinels upon Heat Treatment. In the Figure 3a, the endothermic peaks located at 129−134 °C are assigned to release of the interlayer water of the HTlc phase[17,32] while the peaks at 185−205 °C can be attributed to the dehydration of O−H groups (i.e., the collapse of the HTlc phase).[15,23] The broad endothermic bands at 243−249 °C are attributable to the decomposition of anion species in the solid.[15,23,32] This assignment is supported with IR observation that the intensities for anion vibrational modes for the calcined samples are reduced significantly over the temperature range studied. Because of the presence of brucite-like sample in sample A75, there is a large peak observed at 299 °C.[15,23,32] Apparently this huge endothermic peak overlaps the anion decomposition band which is located at the low-temperature part of the peak. A small endothermic peak at 71 °C in A100 can be attributed to surface-adsorbed water, noting that a small phase of the oxide spinel has been formed in this sample.

In the sample series B (Figure 3b), the HTlc in samples B25 and B50 is poorly crystallized, or small-sized, judging from the diffraction peak widths in the XRD patterns (Figure 1b). In view of the small-sized crystallites in these samples, it is believed that the depletion of intercalated water can be eased, which may explain why there is no well-defined band (only shows a slope before 150 °C) for the interlayer water depletion. The large endothermic peak at 160 °C in sample B25 can be attributed to the dehydration of O−H,[15,23] while the second peak at 213 °C can be attributed to the anion decomposition in the HTlc phase.[15,23,32] With increase in Mg content, the above two peaks move toward higher

(27) Busca, G.; Trifiro, F.; Viccari, A. *Langmuir* **1990**, *6*, 1440.
(28) Xu, Z. P.; Zeng, H. C. *Chem. Mater.* **1999**, *11*, 67.
(29) Grey, I. E.; Ragozzini, R. *J. Solid State Chem.* **1991**, *94*, 244.
(30) Ulibarri, M. A.; Hernandez, M. J.; Cornejo, J. *J. Mater. Sci.* **1991**, *26*, 1512.
(31) Lutz, H. D.; Feher, M. *Spectrochim. Acta A* **1971**, *27*, 357.
(32) Pesic, L.; Salipurovic, S.; Markovic, V.; Vucelic, D.; Kagunya, W.; Jones, W. *J. Mater. Chem.* **1992**, *2*, 1069.

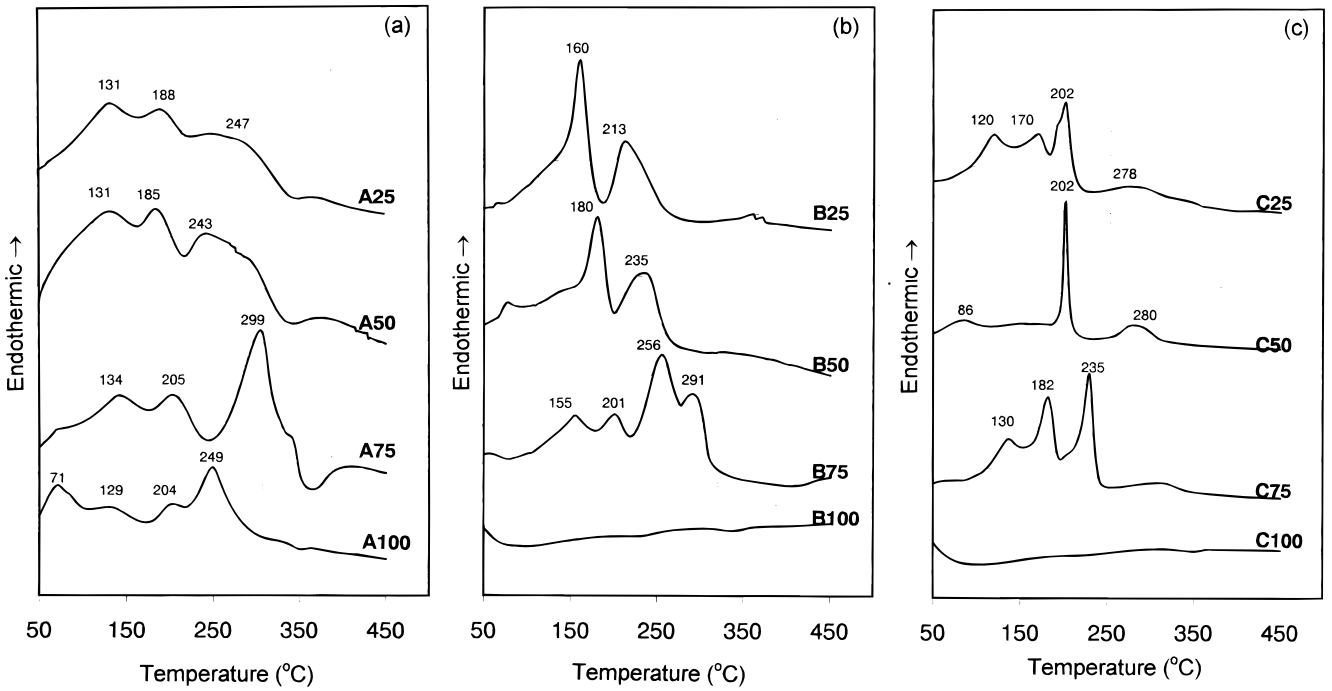

Figure 3. DSC curves for the as prepared precursor samples: (a) A series, (b) B series, and (c) C series.

temperature range (180 °C and 235 °C, respectively) in the sample B50. The FTIR investigation on the calcined samples of this series also leads to the same conclusion for the above thermal event assignments that the spinel phase formed before 200 °C (i.e., collapse of HTlc phase) and a substantial reduction in anion species after 300 °C calcination. However, with increase in Mg content, as in the sample B75, the endothermic peak corresponding to interlayer water depletion locates at 155 °C while the peaks for O−H dehydration and anion decomposition move further to 201 and 256 °C, respectively. Since this sample contains also brucite-like phase, the peak at 291 °C is assigned unambiguously to the dehydration of O−H groups in the brucite-like compound (as in A75).[15,23,32]

DSC scans shown in Figure 3c for the series C are quite different from those of the above two series. In particular, a sharp peak at 202 °C for the turbostratic phase samples C25 and C50 can be identified, which is attributable to the dehydration of O−H groups while the high-temperature peaks at 278−280 °C can be assigned to the decomposition of anion in the solids.[15,23,32] Because the interlayer spacing in turbostratic phase is large, the low-temperature thermal events (86 °C and a flat band in C50; 120 °C and 170 °C in C25) in the two samples are assigned to the adsorbed surface water and interlayer water, respectively. The endothermic peaks at 130, 182, and 235 °C of C75 sample can be assigned respectively to the thermal events for depletion of interlayer water, dehydration of O−H, and decomposition of anions in the HTlc phase.[15,23,32] A small shoulder at around 202 °C can be assigned to the presence of trace of turbostratic phase in this sample, since the $(002)_T$ diffraction is still detectable in XRD pattern (Figure 1c). There is no major thermal event shown in the DSC scan of C100 sample, which reveals that the formation of Co_3O_4 phase has been completed during the hydrothermal synthesis, leaving no unreacted chemical entities in the solids. The thermal events reported for this series are also validated with FTIR spectrum evolutions of anions species and spinel phase in their respective calcined samples at 100−400 °C. In the TGA investigation, the major weight losses are corresponding to the above decomposition assignments, since peaks of the first-order derivatives (with respect to time) of the TGA curves match nicely with the major thermal events revealed in the DCS study (Figure 3).

It has been known that the formation of the spinel phase from the Mg−Co hydroxide nitrate compounds cannot be regarded as a solid-state reaction between two or more active reactants appearing during the thermal decomposition.[2,5] As revealed in an investigation using transmission electron microscopy and selected area electron diffraction experiments, the transformation of Mg−Co hydroxide nitrate compounds to the spinel products is a topotactic process,[2,5] in which metal ions undergo a diffusionless transformation to the spinel phase. For the final spinel products the general chemical formula can be written as $Mg_xCo_{1-x}Co_2O_4$ in which some of Co^{2+} ions are replaced with Mg^{2+}. In an idealized topotactic transformation, one-third of the metal ions in the hydroxide precursors will change their octahedral coordination to tetrahedral, i.e., keeping their original statistical distribution.[2,5] Due to this diffusionless topotactic transformation, a partially inverse spinel structure is expected since the Co/Mg ratio should be the same in both tetrahedron sites and octahedron sites. Thus, the cationic distribution in the respective tetrahedron sites (Td) and octahedron sites (Oh) can be expressed as $(Mg_{x-\gamma}^{2+}Co_{1-x}^{2+}Co_{\gamma}^{3+})^{Td}[Mg_{\gamma}^{2+}Co_{2-\gamma}^{3+}]^{Oh}O_4$, where γ is the degree of inversion. The theoretical values of γ are listed in Table 1 for the studied samples.

FTIR analysis in the current work also confirms the topotactic transformation of the mixed-metal hydroxides to the spinel phase. Both shape and position (wavenumber) of the two characteristic peaks of spinel phase are not changed for every precursor sample heated from 100 to 400 °C (see Experimental Section), which suggests

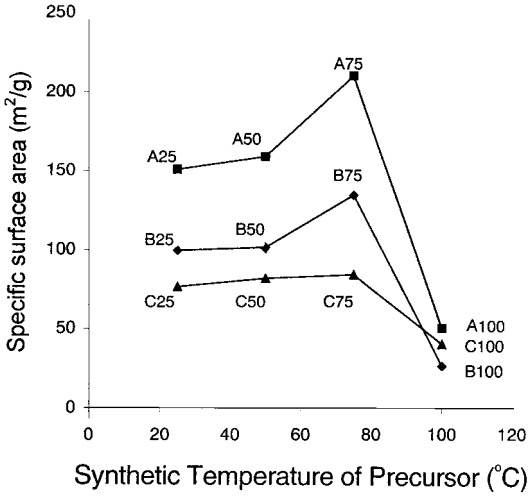

Figure 4. Specific surface area (S_{BET}) profile versus hydrothermal treatment temperature for the as prepared precursor compounds after calcined at 400 °C for 2 h.

that there is no progressive reduction of the inversion degree in the spinel structure upon calcination.[33]

XRD investigation on the 400 °C calcined samples confirms that the prepared catalysts are all in cubic spinel phase,[2,5−7] although their peaks in diffraction patterns are generally broad and weak except those of B100 and C100 (which contain no Mg). Figure 4 presents the BET results for these spinel oxides that will be used in catalytic activity testing. The general trend observed here is that the specific surface area S_{BET} increases with Mg content in the spinel catalyst. The series A gives the largest S_{BET} while the series C the smallest. Furthermore, the S_{BET} increases with rise in hydrothermal treatment temperature over the range of 25−75 °C with a maximum at 75 °C for each series. In particular, the sample A75 ($Mg_{0.91}Co_{0.09}Co_2O_4$ or $(Mg_{0.30}^{2+}$-$Co_{0.09}^{2+}Co_{0.61}^{3+})^{Td}[Mg_{0.61}^{2+}Co_{1.39}^{3+}]^{Oh}O_4$, Table 1) has a S_{BET} = 210 m^2/g (400 °C). Although the Mg content in A75 is the highest among all samples, it is still substoichiometric (x = 0.91) to the form of pure spinel $MgCo_2O_4$ (x = 1.00). It is believed that the substoichiometry and low-temperature calcination prevent the sample from recrystallization, which can be a key to reserve high S_{BET}. To the best of our knowledge, this is the highest surface area achieved so far for the $MgCo_2O_4$ spinel using coprecipitation methods. For example, a S_{BET} = 53 m^2/g (300 °C) was reported for the similar Mg−Co oxide spinels, whose precursor compounds were prepared with sodium hydroxide solution.[5] The 100 °C prepared samples give the lowest S_{BET} within the same series of samples. The S_{BET} data for B100 and C100 are quite similar since they are obtained from the similar Mg-free spinel oxide of cobalt.

Causes for Low-Temperature Formation of $Mg_xCo_{1-x}Co_2O_4$ Spinels. On the basis of the above materials characterization, it is noted that a 100% conversion of the Mg−Co hydroxides to $CoCo_2O_4$ can be attained in the samples B100 and C100 (anhydrous) without postsynthesis calcination. Within the same series of samples, as mentioned earlier, their initial precipitates are the same (prepared at 25 °C). The mole ratio of Co/Mg decreases with respect to the aging

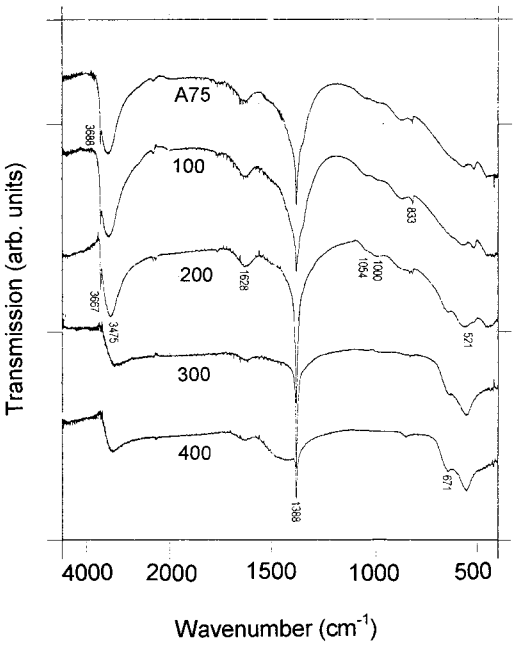

Figure 5. Sequential FTIR spectra for A75 sample after heating at 100, 200, 300, and 400 °C (marked with numbers) for 2 h with respect to the major endothermic events of DSC for this sample (refer also to A75 in Figure 3a).

temperature, which means relative content of Mg in the solid samples is increased (Table 2). However, at 100 °C, the relative Mg content undergoes an abnormal drop (Co/Mg = 8.1 for A100 and the Mg content is virtually zero in both B100 and C100). This reveals that before formations of $Mg_{0.33}Co_{0.67}Co_2O_4$ in the sample of A100 and $CoCo_2O_4$ in B100 and C100 there is a sudden dissolution (or leaching) of Mg from their respective Mg−Co hydroxides at 100 °C. This Mg-leaching depends on the initial Mg^{2+} concentration in the solution. For example, the Mg content is still detectable in the sample of A100 (initial solution concentration ratio of $[Mg^{2+}]$:$[Co^{2+}]$ = 2:1), whereas it is undetectable in the B100 and C100 in which the $[Mg^{2+}]$:$[Co^{2+}]$ = 1:1 and 1:2, respectively. Because of low or no Mg ions in these samples, thermal stability of the metal hydroxides becomes lower,[9] which in turn allows an early decomposition of the hydroxides. Under the present experimental conditions, it is found that a spinel phase can be formed at >50 °C inside the solution if the Co/Mg mole ratio is >8.

As the sample A75 has shown high specific surface in all samples, in Figure 5, FTIR spectrum evolution of this sample will be illustrated to show its thermal conversion process to the spinel phase. For calcined samples over 100−200 °C, a small absorption band located at ∼1054−1000 cm^{-1} can be identified respectively from the two spectra while the width and intensity of 1388 cm^{-1} peak decreases. The bands at 1054−1000 cm^{-1} are commonly assigned to ν_1 mode of NO_3^- due to lowering of anion symmetry from D_{3h} to C_{2v}, as mentioned before.[20,24−26] Since all final products in the three series are $Mg_xCo_{1-x}Co_2O_4$ (x = 0.0 to 0.9) spinels, the thermal decomposition of the solid coprecipitates involves also the oxidation of divalent Co^{2+} to trivalent Co^{3+}, in addition to the existing Co^{3+} in the HTlc phase which has been produced during the synthesis. In this regard, intercalated NO_3^- also acts as an oxidant for

(33) Busca, G.; Lorenzelli, V. *Mater. Chem. Phys.* **1992**, *31*, 221.

the thermal oxidation/decomposition. On the basis of the above FTIR results, conversion of Co^{2+} in the HTlc phase to Co^{3+} can be postulated below:

$$Co^{2+} + NO_3^- = Co^{2+}O^- - NO_2 \quad (1)$$

$$Co^{2+}O^- - NO_2 = Co^{3+}O^{2-}\cdots NO_2 \quad (2)$$

$$Co^{3+}O^{2-}\cdots NO_2 = (CoO)^+ + NO_2(g) \quad (3)$$

Upon heating, which turns 2 OH^- in the brucite-like sheets into a H_2O and an O^{2-}, some Co^{2+} cations become coordinately unsaturated. Equation 1 is thus proposed in view of the observation of nitrato complex vibrations at 1054−1000 cm^{-1}.[20,24−26] Further heating on this Co−ONO_2 pair would lead to an electron transfer form Co^{2+} ($3d^7$) to the end oxygen and weaken the O−N bonding ($Co^{3+}O^{2-}\cdots NO_2$, eq 2). Furthermore, the off-gas released from the sample calcined in a vacuum shows a color of reddish brown (a characteristic of NO_2); eq 3 is thus validated. This postulation is further supported by the observation of distorted NO_3^- monodentate nitrate anion, whose symmetry reduction causes ν_1 mode to become IR active.[34,35] When the HTlc phase is fully decomposed, the bands at 1054−1000 cm^{-1} cannot be detected. In this connection, at higher temperatures (e.g., 400 °C), the bands at 1480 cm^{-1} appear which can be assigned to the symmetric vibration of monodentate nitrate [$\nu_s(ONO_2)$] while the 1388 cm^{-1} peak is significantly reduced.[34,35]

Catalytic Activities of $Mg_xCo_{1-x}Co_2O_4$ Spinels. Kinetic studies of the decomposition of N_2O on low Co-content catalyst system of CoO/MgO (Co = 0.05 atom %) were reported in the 1960s and 1970s.[36,37] The activity per cobalt atom was reported to decrease with increasing Co concentration in MgO.[36,37] Recently MgO-supported CoO had been considered to be the most active catalyst,[38] although a pure phase of Co_3O_4 had also shown excellent activity in our N_2O decomposition study.[15] In the present work, we have introduced Mg into the spinel structure of Co_3O_4 that leads to a significant improvement in catalytic activity for N_2O decomposition. Figure 6 gives conversion data for some representative samples studied at GHSV = 21600−25200 h^{-1}. Although the crystallographic structure for these oxides is unexceptionally in spinel phase as evidenced by XRD for the catalysts before and after nitrous oxide decomposition, their catalytic activity varies substantially due to compositional variation in $Mg_xCo_{1-x}Co_2O_4$. On the weight basis of catalyst, sample series B gives the highest activity, noting that B75 ($Mg_{0.69}Co_{0.28}Co_2O_4$) is the most active one (Figure 6a) and its S_{BET} is also the highest in the series (Figure 4). Although A75 has the highest content of Mg and the highest S_{BET} among all the samples, its catalytic activity is not the highest (Figure 6b). Nevertheless, on the basis of surface area, the catalysts with higher content of Co are still more active. For instance, when comparing the 20% N_2O conversion at 400 °C of catalyst B100 with 70% N_2O conversion at 400 °C of B75, it is clear that the specific activity (per square meter of catalyst) is still higher on the B100. The above observations indicate that while a proper mole ratio of Mg/Co is important to ensure large surface area, Co is a more active species in determining ultimate catalytic activity.

Compared to our previous work,[9] the introduction of oxygen to the sample preparation clearly increases the hydrotalcite-like phase in the precipitates. Moreover, the rise in ratio of [Mg^{2+}]:[Co^{2+}] in the synthesis also increases the Mg content in the precursor solids (A series, Table 1). These two changes have led to the significant increase of specific surface area of the catalysts at higher calcination temperature of 400 °C (Figure 4). Therefore, the effectiveness of the cobalt for the N_2O conversion has been greatly enhanced. Compared with the reported conversion data in the literature, the present $Mg_xCo_{1-x}Co_2O_4$ catalysts should be considered highly active. For example, the conversion activity of catalyst B75 operated at 380−400 °C is in the range of 30.6−38.9 mmol (N_2O)/g·h (GHSV = 21 200 h^{-1}, N_2O = 10 mol % balanced with He), compared to that of 1.6−2.3 mmol (N_2O)/g·h (GHSV = 30 000 h^{-1}, N_2O = 0.1 mol % balanced with He) for an active Co−Mg−Al spinel catalyst (which was derived from the hydrotalcite-like compound Co−Mg−Al HTlc) operated at 350−400 °C.[39,40] It has been evidenced that decomposition of nitrous oxide on metal oxide surface involves an electron transferring from a low oxidation state metal cation to an adsorbed nitrous oxide molecule.[41,42] Related to the present catalyst system, the following mechanism can be proposed for nitrous oxide decomposition:

$$Co^{2+} + N_2O \leftrightarrow Co^{2+}\cdots O - N_2 \quad (4)$$

$$Co^{2+}\cdots O - N_2 \rightarrow Co^{3+}O^- + N_2 \quad (5)$$

$$Co^{3+}O^- \rightarrow Co^{2+} + {}^1/_2\, O_2 \quad (6)$$

where Co^{2+} is a divalent cobalt surface species and $Co^{2+}\cdots O-N_2$ represents adsorbed nitrous oxide species on an active site (eq 4). For many metal oxide catalysts, charge transfer from a low-valence metal cation to the adsorbed N_2O is often considered as fast surface reaction, as proposed in eq 5.[41,42] Due to the site inversion in the spinel structure, as addressed in the above subsections, divalent Co^{2+} and trivalent Co^{3+} both exist in tetrahedral sites, in addition to the Mg^{2+}. Unlike a proposed mechanism that the charge-transfer process of Co^{2+} to Co^{3+} causes the CoO phase to change to Co_3O_4,[38] the coexistence of Co^{2+} and Co^{3+} in 4-fold-coordinated sites requires little geometrical change for the two types of cations in the charge-transfer process. The charge-

(34) Schraml-Marth, M.; Wokaun, A.; Baiker, A. *J. Catal.* **1992**, *138*, 306.
(35) Zotov, N.; Petrov, K.; Dimitrova-Pankova, M. *J. Phys. Chem. Solids* **1990**, *51*, 1199.
(36) Cimino, A.; Bosco, R.; Indovina, V.; Schiavello, M. *J. Catal.* **1966**, *5*, 271.
(37) Cimino, A.; Pepe, F. *J. Catal.* **1972**, *25*, 362.
(38) Drago, R. S.; Jurczyk, K.; Kob, N. *Appl. Catal. B* **1997**, *13*, 69.
(39) Kannan, S.; Swamy, C. S. *Appl. Catal. B* **1994**, *3*, 109.
(40) Armor, J. N.; Braymer, T. A.; Farris, T. S.; Li, Y.; Petrocelli, F. P.; Weist, E. L.; Kannan, S.; Swamy, C. S. *Appl. Catal. B* **1996**, *7*, 397.
(41) Akbar, S.; Joyner, R. W. *J. Chem. Soc., Faraday Trans. 1* **1981**, *77*, 803.
(42) Eley, D. D.; Klepping, A. H.; Moore, P. B. *J. Chem. Soc., Faraday Trans. 1* **1985**, *81*, 2981.

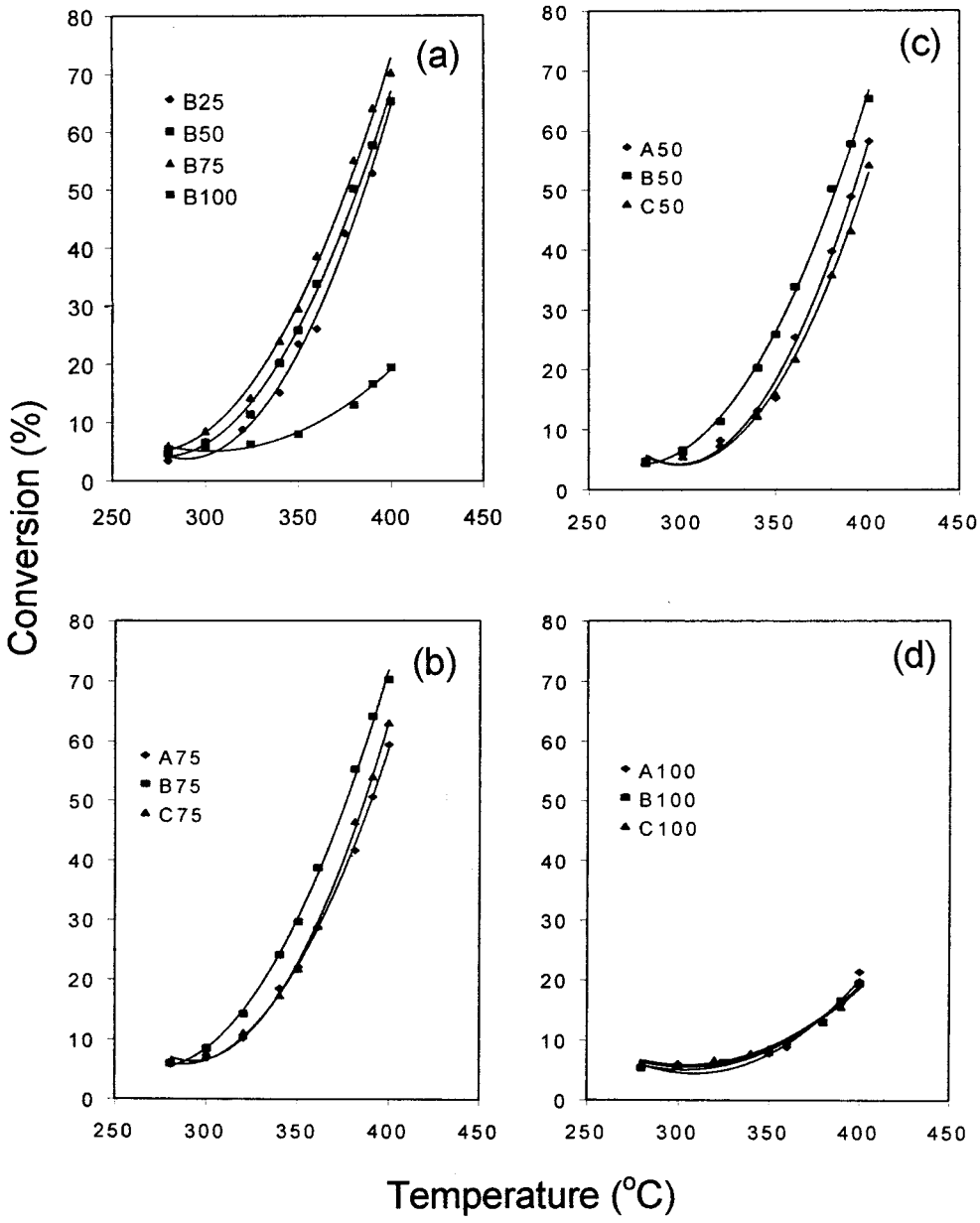

Figure 6. Conversion percentage versus reaction temperature for the studied spinel catalysts prepared from (a) B series of samples, (b) 75 °C aged samples, (c) 50 °C aged samples, and (d) 100 °C aged samples.

transfer product, $Co^{3+}O^-$, can be considered as a 5-fold-coodinated Co^{3+}. Because of the 4-fold requirement for a tetrahedral site, the resultant $Co^{3+}O^-$ species would seemingly return to the divalent Co^{2+} (tetrahedral) by releasing one of the five oxygen anions (eq 6). This proposed mechanism is supported by an ^{18}O isotope labeling investigation which indicates that O from N_2O enters metal oxide catalysts (mordenites) through surface oxygen ion vacancy sites.[43,44] It has been reported that the presence of Mg^{2+} helps N_2O adsorption, which also facilitates the electron transfer from the Co^{2+}. As revealed in the present study, the divalent Mg and Co are mixed at atomic level in the tetrahedral sites. This structural arrangement may be more advantageous for adsorption of N_2O and charge transfer. With a suitable mole ratio between Mg^{2+} and Co^{2+}, active catalysts can be tailor-made for nitrous oxide decomposition at low-temperature.

Conclusions

In summary, the cation ratios of $[Mg^{2+}]:[Co^{2+}]$ and hydrothermal treatment temperature can be used to control the chemical composition, structure, and chemical reactivity of spinels $Mg_xCo_{1-x}Co_2O_4$ ($x = 0.0-0.9$). With an increase in hydrothermal treatment temperature, precursor compounds are changed from the hydrotalcite-like to brucite-like and then to cubic spinel phase for the syntheses with $[Mg^{2+}]:[Co^{2+}] \geq 1$, while they are changed from the turbostratic to hydrotalcite-like and then to cubic spinel phase for $[Mg^{2+}]:[Co^{2+}] < 1$. For $x \leq 1/3$, the $Mg_xCo_{1-x}Co_2O_4$ spinels can be obtained in the temperature range as low as 50−100 °C. In the postsynthesis thermal treatment, the hydrotalcite-like phases decompose at 160−205 °C and 213−256 °C respectively and the brucite-like at ∼291−299 °C, while

(43) Leglise, J.; Petunic, J. O.; Hall, W. K. *J. Catal.* **1984**, *86*, 392.
(44) Valyon, J.; Millman, W. S.; Hall, W. K. *Catal. Lett.* **1994**, *24*, 215.

the turbostratic phase decomposes at 202 °C and 278−280 °C, respectively. On the basis of FTIR results, the topotactic transformation of these precursor compounds to the spinels can be confirmed. Specific surface area as high as 210 m^2/g can be obtained in high Mg content spinel with $x = 0.9$. The easy formation of spinel phase at low-temperature can be attributed to the presence of Co^{3+} and the leaching of Mg^{2+} from the solid phase, while the thermal oxidation of Co^{2+} can also be related to the participation of intercalated NO_3^-. Excellent catalytic activity for N_2O decomposition is attributed to the mixed active sites of Co^{2+} and Mg^{2+} with tetrahedral coordination.

Acknowledgment. The authors gratefully acknowledge research funding (RP960716 and A/C50384) cosupported by the Ministry of Education and the National Science and Technology Board of Singapore.

CM990355L